A computational framework for rheologically complex thermo-visco-elastic materials

P. Lenarda[a,*], M. Paggi[a]

[a]*Research Unit Multi-scale Analysis of Materials (MUSAM), IMT School for Advanced Studies Lucca*

Abstract

Fractional calculus has been proved to be very effective in representing the visco-elastic relaxation response of materials with memory such as polymers. Moreover, in modelling the temperature dependency of the material functions in thermo-visco-elasticity, the standard time-temperature superposition principle is known to be ineffective in most of the cases (thermo-rehological complexity). In this work, a novel finite element formulation and numerical implementation is proposed for the simulation of transient thermal analysis in thermo-rehologically complex materials. The parameters of the visco-elastic fractional constitutive law are assumed to be temperature dependent functions and an internal history variable is introduced to track the changes in temperature which are responsible for the phase transition of the material. The numerical approximation of the fractional derivative is employed via the so called Grnwald-Letnikov approximation. The proposed model is used to numerically solve some test cases related to relaxation and creep tests con-

*Corresponding author. Tel: +39 3337952151, e-mail: pietro.lenarda@imtlucca.it

ducted on a real polymer (Etylene Vynil Acetate), which is used as the major encapsulant of solar cells in photovoltaics.
Keywords: Thermo-visco-elasticity, fractional calculus, materials with memory, finite element method, rheological complexity.

---

1. Introduction

The theory of visco-elasticity deals with the description of materials that exhibit a combination of elastic (able to recover the original undeformed state after stress removal) and viscous (deformation-preserving after stress removal) behaviours. Quantitative description of such materials involves a strain-stress constitutive relation that depends upon time. The classical linearized model of visco-elasticity leads to an integro-differential equation in which the elastic stress tensor $\boldsymbol{\sigma}$ is a convolution product between the strain $\boldsymbol{\varepsilon}$, which encodes the deformation history of the material up to the current time, with an appropriate memory kernel $E(t)$ (in one dimension), representing the relaxation mechanism:

$$\sigma(t) = \int_0^t E(t-s)\dot{\varepsilon}(s)\ \mathrm{d}s. \tag{1}$$

The visco-elastic constitutive response is usually assessed through experimental creep or relaxation tests. In a relaxation test, a constant strain ε_0 is applied quasi-statically to a uniaxial tensile bar at $t = 0$. Due to visco-elasticity, the stress σ needed to maintain the imposed strain decreases with time. The relaxation modulus of the material is defined as $E(t) = \sigma(t)/\varepsilon_0$,

and it usually shows a power-law dependency with time for the majority of polymers. In the creep test, on the other hand, the uniaxial tensile bar is loaded by a constant stress σ_0 imposed at $t = 0$. Again, the load is applied quasi-statically or in such a manner as to avoid inertia effects, and the material is assumed to have no prior history. In this case, the strain ε under the constant load increases with time and the test defines a new quantity called *creep compliance* $J(t) = \varepsilon(t)/\sigma_0$. Various mathematical models have been proposed and used to represent the visco-elastic material functions analytically. The simplest mechanical model consists of two elements: a spring for the elastic behavior and a dashpot for the viscous one. Spring and dashpot elements can be combined in a variety of arrangements to produce a simulated visco-elastic response. Early models due to Maxwell and Kelvin combine a linear spring in series or in parallel with a Newtonian damper [1]:

$$k\sigma + \eta\frac{D\sigma}{Dt} = k\eta\frac{D\varepsilon}{Dt} \quad \text{(Maxwell)}, \tag{2a}$$

$$\sigma = k\varepsilon + \eta\frac{D\varepsilon}{Dt} \quad \text{(Kelvin-Voigt)}. \tag{2b}$$

Other basic versions include the three-parameter solid and the four-parameter fluid models. A more versatile model is obtained by connecting a number N of Maxwell elements (arms) in series and adding a spring in parallel, leading to a Prony series relaxation function:

$$E(t) = E_0 + \sum_{i=1}^{N} E_i \exp(-t/\tau_i), \tag{3}$$

where E_i, τ_i are material properties to be determined from data. It has to be pointed out that E_i, τ_i in the Prony series have to be fitted from real data obtained from realxation tests. This is not a straight forward task because it involves the solution of a constrained optimization problem, as pointed out in [2, 3].

Fractional calculus has been proved to be very effective in modelling the power-law time-dependency of the relaxation behavior of polymers, offering also an easier way to estimate the model parameters as compared to the above rheological models [4–6, 32–35, 38–40]. As highlighted in [7], Nutting, established in 1921 that for many polymers the relationship between stress and strain is described by an equation of the form:

$$\sigma(t) = At^{-\alpha}\varepsilon(t), \quad 0 \leq \alpha \leq 1, \tag{4}$$

where the relaxation modulus $E(t)$ in Eq. (4) is assumed to be a fractional kernel function of the parametres $A > 0, 0 \leq \alpha \leq 1$ of the type:

$$E(t) = At^{-\alpha}/\Gamma(1-\alpha), \tag{5}$$

being $\Gamma(x)$ the Euler gamma function. In this case, the constitutive relation (5) reduces to an elastic spring for $\alpha = 0$ or to a dashpot for $\alpha = 1$, suggesting that visco-elasticity is something in between those two limit constituive models. This is the reason why the stress-strain relation (5) is usually called a spring-pot element [8, 9]. Noting that the fractional derivative of a function

$f(t)$ of order $0 \leq \alpha \leq 1$ is defined as [19]:

$$D^{\alpha} f(t) = \frac{1}{\Gamma(1-\alpha)} \int_0^t (t-s)^{-\alpha} \dot{f}(s) \, \mathrm{d}s, \tag{6}$$

it is straightforward to recast the constitutive relation (5) in terms of a fractional derivative [8, 10–12]:

$$\sigma(t) = A D^{\alpha} \varepsilon(t). \tag{7}$$

Polymers display a strong thermo-visco-elastic constitutive response, with a variation in the material properties up to three orders of magnitude, depending on temperature [2–4, 35, 38–40]. Hence, it is a common assumption the use of the so-called time-temperature superposition principle [1, 13–15], which states that all the material visco-elastic functions at any temperature T can directly be obtained from the same curve, the so-called *master-curve*, obtained at a base temperature T_{ref}, shifted in the time axis by a quantity a_T. This quantity is a material parameter and must be determined from experiments. Unfortunately, for a large class of materials, this fitting leads to poor results showing that the time-temperature superposition principle does not always apply [2, 3]. Those materials are called thermo-rheologically complex [6, 13].

In the present study, a new formulation for the analysis of coupled thermo-visco-elastic material problems is proposed within the finite element method

that is able to account for rheologically complex materials. For such materials, the classical time-temperature superposition principle does not apply and a fractional calculus formulation, with parameters function of temperature, is developed. A new material function $\tau(t, T)$ is introduced, function of time and temperature history and taking into account the phase transition in the microstructure of the polymer due to temperature variations. Ethylene-Vynil-Acetate (EVA) is considered as a representative material showing this effect in technological applications.

In Section 2, visco-elastic constitutive equations in $3D$ are formulated, with special regard to rheologically complex materials. In Section 3, the strong and weak problems of the thermo-visco-elastic dynamics are formulated. In Section 4, the finite element formulation is derived. Section 5 addresses a series of benchmarks numerical examples to show the capabilities of the presented model. Section 6 concludes this article, highlighting the major results and the future perspectives of the present research.

2. Visco-elastic constitutive equations in 3D and rheologically complex materials

In three dimensions, the material functions characterizing completely the response of a visco-elastic solid are the Young modulus $E(t)$, the bulk modulus $K(t)$ and the shear modulus $G(t)$. The Young modulus is considered to be of fractional type (5), as in [4]. Following [16], the assumption of constant bulk modulus $K(t) = K$ is made. This is because polymer materials are

known to show a predominant visco-elastic behaviour in shear deformation rather than in volumetric expansion. The remaining shear modulus $G(t)$ is found via elastic/visco-elastic correspondence principle and inverse Laplace transform using the Mittag-Leffler special functions [17]. Let us consider a material occupying a region $R \subset \mathbb{R}^3$ in the three-dimensional space. Let $\mathbf{u}$ be the displacement field. Let $\boldsymbol{\varepsilon} = (\nabla \mathbf{u} + \nabla \mathbf{u}^{\mathrm{T}})/2$ be the infinitesimal strain tensor. Assume that the material is isotropic, then decomposing the overall stress tensor $\boldsymbol{\sigma}$ into its deviatoric and hydrostatic parts, a visco-elastic behavior only for the deviatoric part is herein considered. The split of the stress tensor $\boldsymbol{\sigma}$ reads:

$$\boldsymbol{\sigma}_{\mathrm{d}}(t) = 2 \int_0^t G(t-s) \frac{\partial \boldsymbol{\varepsilon}_{\mathrm{d}}(s)}{\partial t} \, \mathrm{d}s, \quad \boldsymbol{\sigma}_{\mathrm{v}}(t) = 3K \boldsymbol{\varepsilon}_{\mathrm{v}} \tag{8}$$

where $\boldsymbol{\sigma}_{\mathrm{d}} = \boldsymbol{\sigma} - \boldsymbol{\sigma}_{\mathrm{v}}/3$ and $\boldsymbol{\varepsilon}_{\mathrm{d}} = \boldsymbol{\varepsilon} - \boldsymbol{\varepsilon}_{\mathrm{v}}/3$ are the deviatoric stress and strain tensors, $G(t)$ is the shear modulus and $K(t) = K$ is the constant bulk modulus. The visco-elastic constitutive model (8) is of Kelvin-Voigt type. To solve the three-dimensional visco-elastic problem, it is necessary to know the actual mathematical expression of the three material functions G, K and E, and their dependency upon time. Following [4], a Young modulus of fractional type is herein considered:

$$E(t) = At^{-\alpha}/\Gamma(1-\alpha), \quad 0 \leq \alpha \leq 1. \tag{9}$$

Given the espression of the Young modulus $E(t)$, an explicit time-dependency of the shear modulus $G(t)$ is now obtained. Let f be a function and denote with $\mathcal{L}[f]$ its Laplace transform. The s-multiplied Laplace transform given by $s \cdot \mathcal{L}[f]$ is denoted as $\overline{f}^*(s)$. The elastic/visco-elastic correspondence principle [18] states that, in the Laplace domain, the shear modulus is given by:

$$\overline{G}^*(s) = \frac{3\overline{E}^*(s)\overline{K}^*(s)}{9\overline{K}^*(s) - \overline{E}^*(s)}, \tag{10}$$

then, because $K(t) = K$ and $E(t)$ is given by Eq. (9), in the Laplace domain $K(s) = K/s$ and $E(s) = As^{\alpha-1}$. Substituting these espressions in Eq. (10) and taking the inverse Laplace transform, leads to:

$$G(t)/3 = -E_\alpha[-9Kt^\alpha/A],$$

where

$$E_\alpha[x] = \sum_{k=0}^{\infty} \frac{x^k}{\Gamma(\alpha k + 1)}$$

is the Mittag-Leffler special function of order α [17, 19]. Since this function does not have a closed-form expression, the following asymptotic approximation is introduced:

$$E_\alpha[-\lambda t^{-\alpha}] \approx \begin{cases} 1 - \lambda \dfrac{t^\alpha}{\Gamma(1+\alpha)}, & t \to 0^+ \\ \dfrac{t^{-\alpha}}{\lambda\Gamma(1-\alpha)}, & t \to +\infty, \end{cases} \tag{11}$$

valid for any λ. From this expression, the formula found by Pipkin in [20] is recovered:

$$G(t) \approx E(t)/3, \quad t \to +\infty, \tag{12}$$

which will be used in the sequel as the expression for the time-dependent shear modulus.

2.1. Time-temperature superposition principle and its limits

In treating problems involving polymers, the so-called time-temperature superposition principle is a common assumption. This principle states that all the relaxation functions $E(t,T), G(t,T)$ and $K(t,T)$ at any temperature T can directly be obtained from the material functions at base temperature T_{ref}, by replacing the current time t with a shift function a_T, which is a material property of the material and must, in general, be determined experimentally [21–23, 35, 38–40]:

$$E(t,T) = E(t/a_T, T_{\text{ref}}). \tag{13}$$

This is equivalent to say that, for any fixed temperature T, the relaxation curve $t \mapsto E(t,T)$ is obtained from the same master-curve at a base temperature T_{ref}, shifted along the horizontal axis by a quantity a_T in a log time scale. The shift factor a_T is usually described by the WLF (Williams-Landel-Ferry) equation [24, 25] $\log(\mathrm{a_T}) = -\mathrm{C_1}(\mathrm{T} - \mathrm{T_g})/(\mathrm{C2} - (\mathrm{T} - \mathrm{T_g}))$, where C_1, C_2 are

constants and T_g is the glass transition temperature. The previous espression is known to be valid only for $T > Tg$.

Materials where the shifting results in a satisfactory mastercurve are called thermo-rheologically simple. Unfortunately, this is not the case for several materials, like for instance EVA (Ethylene-Vynil-Acetate), which is a copolymer containing semicrystalline parts and whose microstructure changes with temperature, udergoing several phase transitions [4, 26]. Those materials are called thermo-rheologically complex [7]. The relaxation curves of the Young modulus $E(t, T)$ for EVA at different temperatures in a log-log scale are shown in Fig.1 [2, 4]. It can be noticed that the straight lines have different slopes in the temperature range under consideration, so that an horizontal shifting of the material function $E(t, T)$ for different temperatures T does not result in a satisfactory overlap. This result suggests that the shift factor a_T for the EVA material, as assumed by the time-temperature principle and described by Eq. (13) is not accurate. This issue is confirmed looking at Fig.2 where the fitting of the shift factor (13) for EVA taken from [26] shows a very poor result, suggesting that a refined model should be considered for materials that do not obey the time-temperature superposition principle.

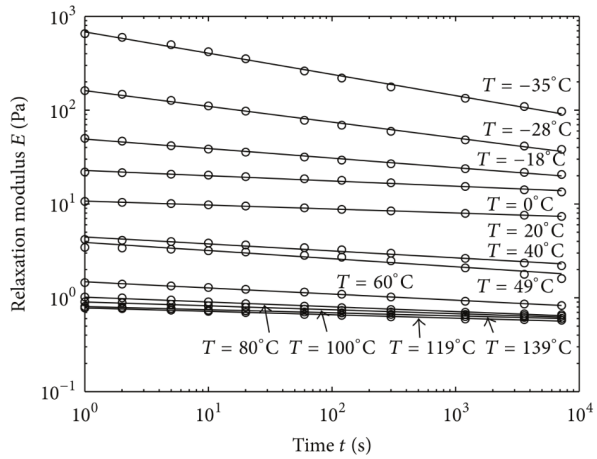

Figure 1: Experimental results of the Young modulus $E(t,T)$ over time in a log-log scale obtained from relaxation tests at different temperatures in a range between $-35°C$ and $139°C$ (dot lines) and results of the fitting according to Eq. (14) (solid lines).

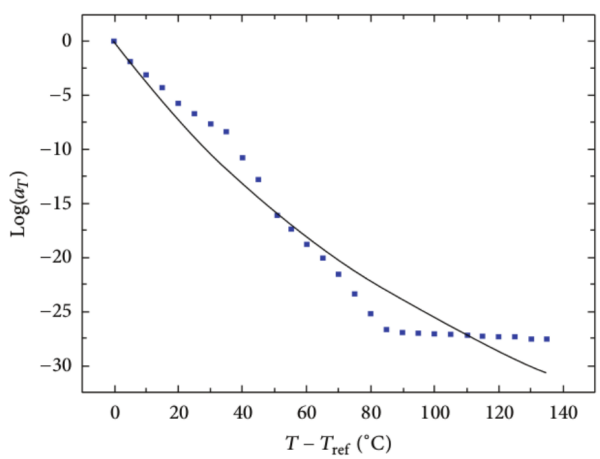

Figure 2: Fitting obtained from experimental results of the shift factor a_T (continuous line) for EVA (Etylen-Vynil-Acetate) using the WLF equation (dot line).

2.2. A new model for thermo-rehological complexity

Following [4], a temperature dependency of the Young modulus is assumed as:

$$E(t,T) = A(T)t^{-\alpha(T)}/\Gamma(1-\alpha(T)), \tag{14}$$

where the material parameters $\alpha(T)$ and $A(T)$ are now temperature dependent. Functions $\alpha(T)$ and $A(T)$ can be determined from Eq. (14), fitting data from uniaxial relaxation tests conducted for different temperatures. Using the asymptotic representation of the shear modulus in Eq. (12), and substituing it in the first of Eqs. (8), leads to the following integral, describing the relaxation behavior of the material properties induced by thermal effects:

$$\frac{A(T)}{\Gamma(1-\alpha(T))}\int_0^t (t-s)^{-\alpha(T)}\frac{\partial \boldsymbol{\varepsilon}_{\mathrm{d}}(s)}{\partial s}\ \mathrm{ds}. \tag{15}$$

This espression is not convenient for applications because both $\alpha(T)$ and $A(T)$ change continuously with temperature T and time t during the process, while it is better to find an espression similar, but having constant values of α and A as long as the internal micro-stucture of the polymer remains the same. To this purpose, a thermal material clock function is defined and an espression similar to (15), which is suitable for applications, is introduced. Consider an arbitrary temperature history $T(t)$, depending on the thermo-visco-elastic process, let $\delta > 0$ be a given threshold. Let $\tau = \tau(t, T)$ be a function which is always smaller or equal to the current time t, which has the role of monitoring the temperature history inside the material. This function is nothing but a counter taking discrete values $0 = \tau_0, \ldots, \tau_k, \ldots,$ that ticks when the temperature variation exceeds the threshold δ. At the beginning of the process, $\tau = \tau_0 = 0$, and it remains zero untill the temperature variation inside the material does not exceed δ. After that moment, the clock ticks

and τ is set equal to a new value $\tau = \tau_1$. In general, during the evolution of the process, there can be several of those temperature jumps, so that the value $\tau(t, T)$ at any time t is defined recursively as:

$$\begin{cases} \tau_0 & = 0 \\ \tau_k & = \inf_{\tau_{\mathrm{k}-1} \leq \mathrm{t}' \leq \mathrm{t}} \{|\mathrm{T}(\mathrm{t}') - \mathrm{T}(\tau_{\mathrm{k}-1})| \geq \delta\}. \end{cases}$$

Consider the reduced time defined as: $\tau(t, T) = \tau_k 1_{[\tau_k, t)}(t)$, where $1_{(a,b)}$ is the indicator function of a (time) interval (a, b). The function $\tau(t, T)$ becomes now a step function, which is constant inside each interval $[\tau_{k-1}, \tau_k]$. The modified material functions are defined as $\tilde{A} = A(T(\tau)) = A(\tau_k) 1_{[\tau_k, t)}$ and $\tilde{\alpha} = \alpha(T(\tau)) = \alpha(\tau_k) 1_{[\tau_k, t)}$, which are constant inside each interval $[\tau_{k-1}, \tau_k]$. The modified relaxation kernel $g_{A,\alpha}(t)$ is defined as:

$$g_{A,\alpha}(t) = \tilde{A}(t - \tau)^{-\tilde{\alpha}} / \Gamma(1 - \tilde{\alpha}).$$

This physical observation suggests that the thermo-visco-elastic relaxation process (15) can be described by the following fractional-thermal derivative:

$$D_{A,\alpha} \boldsymbol{\varepsilon}_{\mathrm{d}}(t) = \int_0^t g_{A,\alpha}(t - s) \dot{\varepsilon}_{\mathrm{d}}(s) \, \mathrm{ds}. \tag{16}$$

Formula (16) basically says that when the variation of temperature inside the material exceeds a given threshold δ, and the thermal clock $\tau = \tau_k$ ticks, the relaxation process is shifted backwards in time of a quantity $t - \tau_k$ and

restarts with new parameters evaluated at $\alpha(T(\tau_k))$ and $A(T(\tau_k))$ for all subsequent times (see Fig. 3). This is because the material has experienced a phase transition and temperature has affected its internal microstructure.

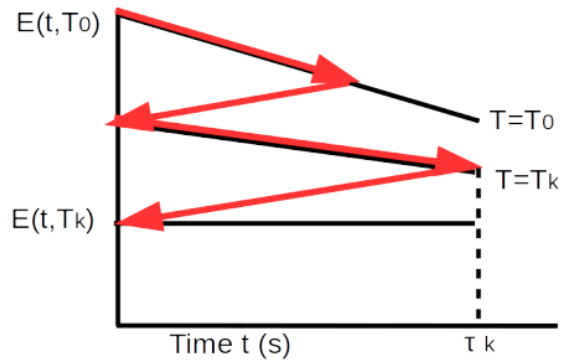

Figure 3: Schematic representation of the relaxation process of the material function $E(t,T)$ depending on the thermal history in a thermo-rheologically complex material.

Accordingly, the relaxation process for a thermo-rheologically complex material can be re-written as:

$$\boldsymbol{\sigma}_{\mathrm{d}} = \frac{2}{3}\int_0^t g_{A,\alpha}(t-s)\dot{\varepsilon}_{\mathrm{d}}(s)\ \mathrm{d}s = D_{A,\alpha}\boldsymbol{\varepsilon}_{\mathrm{d}}(t).$$

Notice that, if the process is adiabatic, i.e. the temperature $T(t)$ remains constantly equal to the initial temperature T_0 during the time interval $[0, t_{\mathrm{fin}}]$, then $\tilde{\alpha} = \alpha(T_0) = \alpha$ and $\tilde{A} = A(T_0) = A$ are constants, the thermal clock is $\tau(t) = 0$, so that $D_{A,\alpha}\varepsilon_{\mathrm{d}}(t)$ reduces to the usual fractional derivative:

$$AD^{\alpha}\varepsilon_{\mathrm{d}}(t) = \frac{A}{\Gamma(1-\alpha)}\int_0^t (t-s)^{-\alpha}\dot{\varepsilon}_{\mathrm{d}}(t)\ \mathrm{d}s.$$

As a concluding remark, the problem of defining an estimate for the threshold δ is adressed. This parameter defines a temperature interval in which the material properties A and α are constants. Looking at Fig. 2, it can be noticed that the slopes of the straight lines are the same in different temperature intervals, i.e., in $[-35°C, -28°C]$, $[-18°C, 20°C]$, $[40°C, 139°C]$. For each of those temperature intervals, one can identify different values of α and A, and a threshold δ can be defined accordingly, to mark the transition from a temperature interval to another.

3. Strong and weak form of the coupled thermo-visco-elastic problem

The deviatoric and hydrostatic parts of the stress tensor are given by:

$$\boldsymbol{\sigma}_{\mathrm{d}}(t,T) = \frac{2}{3} D_{A,\alpha} \boldsymbol{\varepsilon}_{\mathrm{d}}(t),$$
$$\boldsymbol{\sigma}_{\mathrm{v}}(t,T) = 3K\boldsymbol{\varepsilon}_{\mathrm{v}} - 3\beta(T - T_0),$$

where β is the coupling thermal stress factor and T_0 is the initial tempertaure inside the material. Accordingly, the overall stress tensor is given by:

$$\boldsymbol{\sigma}(t,T) = \frac{2}{3} D_{A,\alpha} \boldsymbol{\varepsilon}_{\mathrm{d}}(t) + 3K\boldsymbol{\varepsilon}_{\mathrm{v}} - 3\beta(T - T_0)\mathbf{I}. \tag{17}$$

The balance of linear momentum takes the form:

$$\rho \mathbf{u}_{tt} - \mathrm{div}(\boldsymbol{\sigma}) = 0, \quad (\mathbf{x}, t) \in R \times [0, t_{\mathrm{fin}}], \tag{18}$$

where ρ is the density of the material. Regarding the heat conduction process, the standard Fourier law is assumed for the heat flux $\mathbf{q} = -k\nabla T$, where k is the thermal conductivity. Accordingly, the heat conduction equation reads:

$$k\nabla^2 T = \rho c T_t + \beta T_0 \frac{\partial \varepsilon_{\mathrm{v}}}{\partial t}, \quad (\mathbf{x}, t) \in R \times [0, t_{\mathrm{fin}}], \tag{19}$$

where c is the heat capacity of the material. Eqs. (17), (18) and (19) represent the system of equations for coupled linear thermo-visco-elasticity [27, 28].

The weak form corresponding to the equation of linear momentum (18) is derived by multiplying it by a virtual displacement $\mathbf{v}$ and integrating the result on the domain R. Applying the divergence theorem:

$$\begin{aligned}\int_R \rho\, \partial_{tt}\mathbf{u} \cdot \mathbf{v}\, \mathrm{d}\mathbf{x} + \int_R \frac{2}{3} D_{A,\alpha} \boldsymbol{\varepsilon}_{\mathrm{d}}(\mathbf{u}) : \boldsymbol{\varepsilon}(\mathbf{v})\, \mathrm{d}\mathbf{x} \\ - \int_R \Big(K \mathrm{div}(\mathbf{u}) + \beta(T - T_0) \Big) \mathrm{div}(\mathbf{v})\, \mathrm{d}\mathbf{x} = \int_\Gamma \overline{\mathbf{t}} \cdot \mathbf{v}\, \mathrm{d}\Gamma.\end{aligned}$$

Analogously, the weak form corresponding to the heat conduction partial differential equation (19) is obtained by multiplying it for a test function s and integrating the result over R

$$\int_R k\nabla T \cdot \nabla s\, \mathrm{d}\mathbf{x} + \int_R \rho c \partial_t T s\, \mathrm{d}\mathbf{x} + \int_R \beta T_0\, \mathrm{div}(\partial_t \mathbf{u}) s\, \mathrm{d}\mathbf{x} + \int_\Gamma \overline{q}_n s\, \mathrm{d}\Gamma = 0$$

where the q_n is the imposed normal heat flux $\nabla T \cdot \mathbf{n} = \overline{q}_n$ imposed on the Neumann part of the domain.

4. Finite element formulation

Regarding the finite element formulation, consider a decomposition of the domain R into a finite number of elements and let $\{\mathbf{\Phi}_k^u\}_{k=1}^N$ and $\{\Phi_k^T\}_{k=1}^N$ basis of shape functions. At the element level, the displacement and temperature are interpolated as:

$$\mathbf{u}(\mathbf{x},t) = \sum_{k=1}^{N} \mathbf{\Phi}_k^u(\mathbf{x})\mathbf{U}_k(t), \quad T(\mathbf{x},t) = \sum_{k=1}^{N} \Phi_k^T(\mathbf{x})\mathbf{T}_k(t).$$

Discretizing the time interval $[0, t_{\text{fin}}]$ into $0 = t_0 \leq \cdots \leq t_n \leq t_N = t_{\text{fin}}$ where $t^{n+1} = t^n + \Delta t$ the system of equations is:

$$\mathbf{M}\frac{D^2}{Dt^2}\mathbf{U}^{n+1} + \mathbf{C}^{u,T}\mathbf{T}^{n+1} + \mathbf{G}D_{A,\alpha}\mathbf{U}^{n+1} + \mathbf{K}^u\mathbf{U}^{n+1} = \mathbf{F}, \tag{20}$$

and

$$\mathbf{C}\frac{D}{Dt}\mathbf{T}^{n+1} + \mathbf{C}^{T,u}\frac{D}{Dt}\mathbf{U}^{n+1} + \mathbf{K}^T\mathbf{T}^{n+1} + \mathbf{Q} = \mathbf{0}, \tag{21}$$

where the global matrices and vectors result from the usual assembling of matrices at the element level. In particular, $\mathbf{M}$ is the mass matrix, $\mathbf{C}^{u,T} = (\mathbf{C}^{T,u})^{\mathrm{T}}$ is the coupling thermo-mechanical matrix, $\mathbf{G}$ and $\mathbf{K}^u$ are the shear and bulk matrices and $\mathbf{F}$ is the load vector, $\mathbf{C}$ is the termal dumping matrix, $\mathbf{K}^T$ is the thermal stiffnes matrix and $\mathbf{Q}$ is the thermal loading vector.

The problem of approximating the fractional derivative $D_{A,\alpha}\mathbf{U}^{n+1}$ in Eq. (20) is now adressed. Let $f(t)$ be a function defined in an interval $[0, t_{\text{fin}}]$ and let $0 = t^0 \leq \cdots \leq t^n \leq t^N = t_{\text{fin}}$ be a partition of $[0, t_{\text{fin}}]$, where $t^{n+1} = t^n + \Delta t$. The Grnwald-Letnikov approximation of the fractional derivative $D^\alpha f(t^{n+1})$ of order $0 \leq \alpha \leq 1$ of a f function (see also [9], [30], [19], [5], [29]) reads:

$$\begin{aligned} D^\alpha f(t) &= (\Delta t)^{-\alpha} \sum_{j=0}^{n} c_{j+1}(\alpha) f(t^{n+1-j}) \\ &= (\Delta t)^{-\alpha} \left(f(t^1), \ldots, f(t^{n+1}) \right) \begin{pmatrix} c_{n+1}(\alpha) \\ \vdots \\ c_1(\alpha) \end{pmatrix}, \end{aligned} \tag{22}$$

where the coefficients $c_j(\alpha)$ are defined by the recursive formula:

$$c_j(\alpha) = \begin{cases} \dfrac{(j-1-\alpha)}{j} c_{j-1}(\alpha) & j > 1, \\ 1 & j = 1. \end{cases} \tag{23}$$

Coefficients in Eq. (23) have the properties that $c_j(\alpha) < c_{j+1}(\alpha) < 0$ for $j > 1$ and $\lim_{j \to +\infty} c_j(\alpha) = 0$. Notice that the dimensions of vectors in (22) are increasing with n. Each value $f(t^n)$ up to time t^{n+1} is contribuing to the final value of $D^\alpha f(t^{n+1})$, but the influence of the coefficients is weaker in the past rather than in the present and the initial value $f(t^0)$ is multiplied by $c_{n+1}(\alpha)$, which is tending to zero as n grows. This property of the Grnwald-

Letnikov approximation is called memory effect.

With this set up, the fractional-thermal derivative $D_{A,\alpha}\mathbf{U}^{n+1}$ is approximated as:

$$D_{A,\alpha}\mathbf{U}^{n+1} = A(T^m)(\Delta t)^{-\alpha(T^m)}\left(\mathbf{U}^{n+1} + F_T^m\mathbf{U}^n\right),$$

where $m \leq n$ is a discrete history variable depending on the current time t^n and temperature T^n, taking values $m_0 < m_1 < \cdots < m_k$, defined recursively as $m_0 = 0$ and:

$$m_k = \begin{cases} m_{k-1} & \text{if } |T^n - T^{n-1}| < \delta, \\ n & \text{otherwise} \end{cases}$$

and the operator $F_T^m\mathbf{U}$, collecting the displacement history up to time n, is given by:

$$F_T^m\mathbf{U} = \begin{cases} \displaystyle\sum_{j=m}^{n} c_{n+2-j}(\alpha(T^m))\mathbf{U}^j & \text{if } m < n \\ \mathbf{0} & \text{if } m = n\ . \end{cases} \tag{24}$$

.

Notice that the last term in the sum (24) is $c_2(\alpha(T^m))\mathbf{U}^n$, because the coefficient $c_1(\alpha(T^m)) = 1$ is associated to the unknown vector $\mathbf{U}^{n+1}$. When the process begins, the sum starts to pile up following the Gnwald approximation with material functions $A(T^0)$ and $\alpha(T^0)$ evaluated at the starting temperature T^0, untill the condition $|T^n - T^{n-1}| > \delta$ is verified. After that moment, the history variable m is set equal to n and the process restarts

with new material parameters $A(T^n)$ and $\alpha(T^n)$.

When the process is adiabatic, i.e. the temperature is constant during time, then $m = 0$ for all t^n and $A = A(T_0)$, $\alpha = \alpha(T_0)$, so that the approximation of the thermal-fractional derivative $D_{A,\alpha}\mathbf{U}^{n+1}$ reduces to $AD^{\alpha}\mathbf{U}^{n+1}$, which is exactly the usual Gnwald-Letnikov approximation:

$$AD^{\alpha}\mathbf{U}^{n+1} = A(\Delta t)^{-\alpha}\left[\mathbf{U}^1|\dots|\mathbf{U}^{n+1}\right]\begin{pmatrix} c_{n+1}(\alpha) \\ \vdots \\ c_1(\alpha) \end{pmatrix}.$$

This implies that the displacement history must be stored in a matrix whose number of columnsis progressively increasing and represents the memory of the material. In numerical treatment, the number of columns of the matrix is given by the number of timesteps of the problem and the matrix is initialized to be equal to the zero matrix, then each column is replaced with the displacement solution at the previous timestep.

5. Numerical examples

In this section, several experiments in one and two dimensions are considered to test the new thermo-visco-elastic model which has been introduced in this work.

5.1. Free vibrations of a visco-elastic 1D rod

In this example, the problem of finding the vertical displacement $u(x)$ of a one dimensional visco-elastic vibrating rod of lenght L clamped at its ends $u(0) = u(L) = 0$ is considered, being subjected to an initial sinusoidal prerturbation $u_0(x) = \sin(\pi x)$ at time $t = 0$ and then left free to its own vibration without any external force or traction imposed. The motion of the rod is governed by the following equation which has to be solved in space $0 \leq x \leq L$ and time $0 \leq t \leq T_f$:

$$\rho u_{tt} - \frac{\partial}{\partial x}\left(\frac{A}{\Gamma(1-\alpha)}\int_0^t (t-s)^{-\alpha} u_{xt}(s)\ \mathrm{d}s\right) = 0, \tag{25}$$

where ρ is the linear density of the rod and $A > 0$ and $0 \leq \alpha \leq 1$ are visco-elastic material parameters. Notice that for $\alpha = 0$ this problem reduces to the usual wave equation in one dimension for a linear elastic rod:

$$\rho u_{tt} - A u_{xx} = 0.$$

In the limit case $\alpha = 0$, the mechanical energy of the system is given by:

$$E(t) = \frac{1}{2}\int_0^L \left[\rho\left(\frac{\partial u}{\partial t}\right)^2 + \left(\frac{\partial u}{\partial x}\right)^2\right]\ \mathrm{d}x.$$

A global property of the solution of this problem when $\alpha = 0$ is that $\dot{E}(t) = 0$, i.e. the mechanical energy is conserved. Every numerical method applied to solve this problem must be able to represent this global property of the

solution in the linear elastic limit $\alpha = 0$. Let h be the spatial mesh size, N the number of vertices of the mesh and $\{\Phi_a(x)\}_{a=1}^N$ a basis of linear triangular lagrangian shape functions, then the global $N \times N$ mass and stiffness martices $\mathbf{M}$, $\mathbf{K}$ are explicitely given by the tridiagonal matrices:

$$\mathbf{M} = \rho \begin{pmatrix} \frac{2h}{3} & \frac{h}{6} & \dots & 0 \\ \frac{h}{6} & \frac{2h}{3} & \dots & 0 \\ \vdots & \vdots & \ddots & \vdots \\ 0 & 0 & \dots & \frac{2h}{3} \end{pmatrix}, \quad \mathbf{K} = A \begin{pmatrix} \frac{2}{h} & -\frac{1}{h} & \dots & 0 \\ -\frac{1}{h} & \frac{2}{h} & \dots & 0 \\ \vdots & \vdots & \ddots & \vdots \\ 0 & 0 & \dots & \frac{2}{h} \end{pmatrix}.$$

The nodal displacement vector is given by $\mathbf{U} = (\mathbf{U}^1, \dots, \mathbf{U}^N)^{\mathrm{T}}$ and the differential system arising from the FE discretization is:

$$\mathbf{M}\frac{D^2\mathbf{U}}{Dt^2} + \mathbf{K}D^\alpha\mathbf{U} = \mathbf{0}.$$

In Fig. 4 are shown the evolution in space and time of the numerical solution of the adimensionalized Eq. (25) for two different values $\alpha = 0$ and $\alpha = 0.2$ using a central difference time integration scheme. The parameters used for the simulation are $N_s = 100$ spatial nodes and $N_t = 200$ temporal nodes. Fig. 5 shows the evolution over time of the solution $u(1/2, t)$ for different values of the fractional exponent $\alpha = \{0, 0.1, 0.2, 0.3\}$. The Grnwald-Letnikov approximation of the fractional derivative $D^\alpha\mathbf{U}$ is used, this leads to the formation of a (pseudo-load or forcing) vector $\mathbf{F}^n$ which represents the dislacement history up to the current time. This residual load vector has the

effect of dissipating the mechanical energy of the system, according to the memory effect of the material.

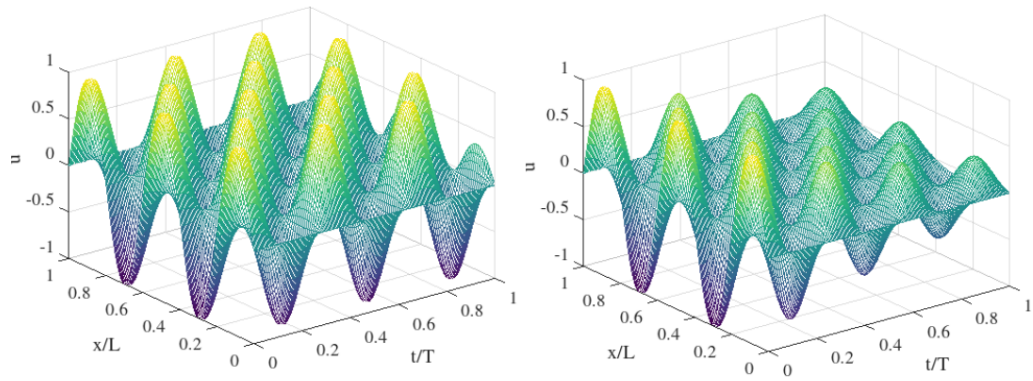

Figure 4: Spatio-temporal plot of the numerical solution of the adimensionalized fractional visco-elastic wave equation for different exponents of the fractional derivative $\alpha = 0$ (linear elastic case) and $\alpha = 0.2$.

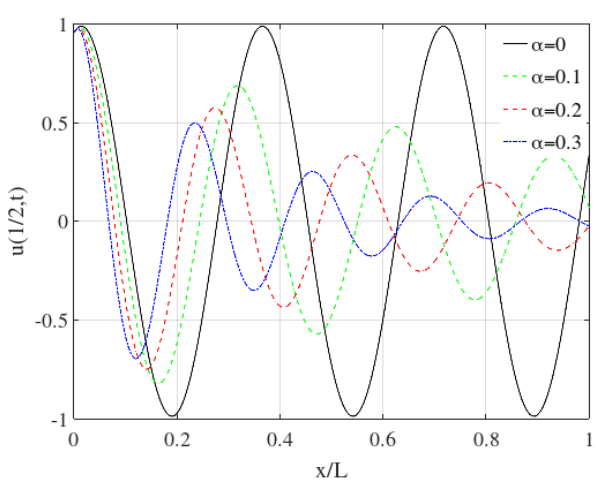

Figure 5: Temporal evolution of the numerical solution of the vertical displacement $u(1/2, t)$ in the $1D$ fractional visco-elastic wave equation for different exponents of the fractional derivative $\alpha = 0$ (solid line) and $\alpha = 0.1, 0.2$ and 0.3 (dashed line).

5.2. Temperature behavior of the relaxation modulus

One of the fundamental tests used to characterize the visco-elastic time-dependent behavior of a polymer is the creep (and creep recovery) test. In a creep test, a constant stress σ_0 is applied quasi-statically to a uniaxial tensile bar at zero time and held constant, as shown in the schematic Fig. 6. The strain, under the constant load, increases with time up to a constant value ε_0. A specimen of size $H \times L$ is clamped on the bottom side and a traction $\mathbf{F}$ is applied on the top of the beam so that $\sigma_0 = ||\mathbf{F}||$. The inertia of the beam is neglected. The variation of the Young's modulus with temperature can be

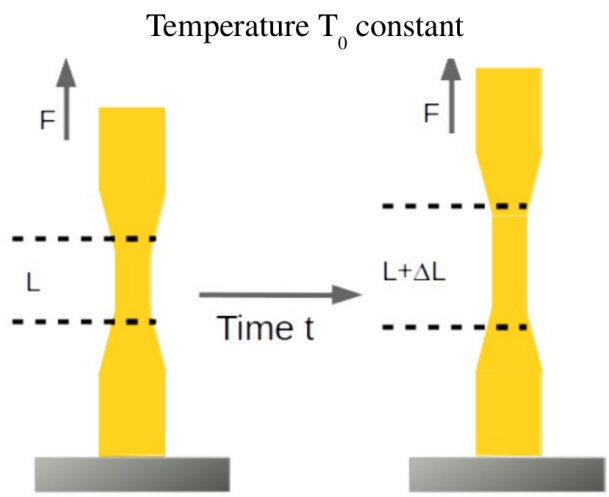

Figure 6: Schematic representation of a creep test.

determined from relaxation and creep tests conducted at different constant temperatures. Material parameters $\alpha(T)$ and $A(T)$ have been experimentally found for a polymeric material, namely Etlylene Vynil Acetate at different temperatures and are taken from [4] as they are reported in Table 1. A

specimen of lateral size $L = 0.02$ m and vertical size $H = 0.08$ m is subjected to a constant traction $\sigma_0 = 500$ N on the top size. During the process, the temperature is held constant $T = T_0$. The Young's modulus is evaluated as:

$$E(t) = \sigma_0/\varepsilon_y(t).$$

Since this process is adiabatic, the Grnwald-Letnikov approximation of the fractional derivative is employed with constant coefficients α and A. Numerical results of the relaxation curves as a function of time $E(t, T)$ obtained for different constant temperatures are reported in Fig. 7 in a log log scale and are in good agreement with the experimental ones in Fig. 1. Input parameters for the simulation are the Poisson coefficient $\nu = 0.29$, the Young modulus $E = 3500$ MPa, the bulk modulus $K = E/3(1 - 2\nu)$ and the constant traction imposed at the upper side of the specimen is $\sigma_0 = 500$ N. The input values of temperatures and corresponding fractional parameters obtained from a best fitting in [4] are reported in Table 1. It is worth noting that, as expected experimentally there is a change in the slope of the curves due to different temperatures, which is a thermo-rehologically complex behaviour of the material. In particular the elastic modulus $E(t, T)$ experiences a phase transition due to the variation of temperature which the proposed model is able to predict.

Table 1: Identified parameters from [4] α and A used in tne numerical simulations of uniaxial relaxation tests at different temperatures.

T_0	α	A [Pa s$^\alpha$]
-28 °C	0.16810	182.7
-18 °C	0.10150	52.63
0 °C	0.05566	23.55
40 °C	0.07417	4.668
60 °C	0.06542	1.544
100 °C	0.04179	0.9276

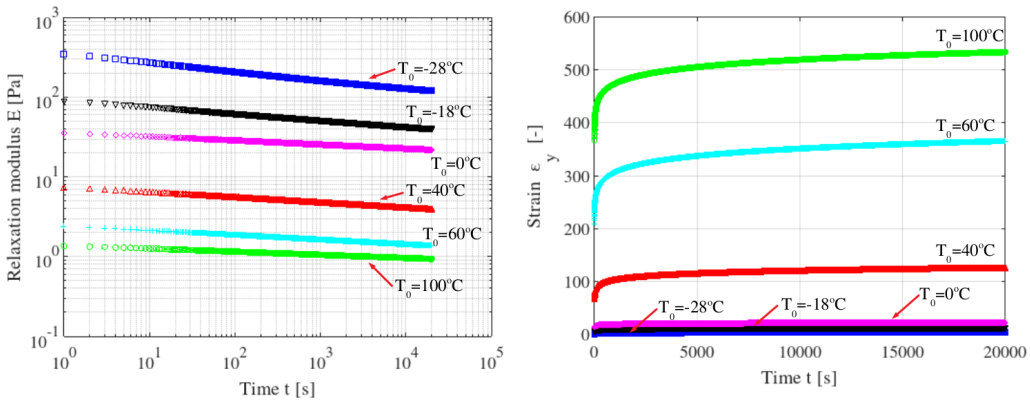

Figure 7: Numerical results obtained from the simulations of the relaxation modulus E (left) and vertical component of the strain ε_y versus time for EVA specimen at different temperatures obtained for fixed temperatures -28 °C, -18 °C, 0 °C, 40 °C, 60 °C, 100 °C.

5.3. The role of truncation in the Grnwald-Letnikov fractional derivative

In this numerical example, the role of truncation in the approximation of the fractional derivative using the Grnwald-Letnikov is investigated. The relaxation test is the same as in the previous example conducted for constant temperatures $T_0 = -28°\text{C}, -18°\text{C}, 0°\text{C}$ with a timestep $\Delta t = 0.1$ s and $T = 80000$ s, which is enough to ensure the stationary convergence of the relaxation process. A parametric study is made by changing the memory

horizon T_{h} to assess the effect of truncation of the fractional derivative.

The memory horizon is varied as $T_{\mathrm{h}} = 20000\ \mathrm{s}, 40000\ \mathrm{s}$. The first part of the process up to time T_{h} follows the Grnwald-Letnikov method. After that, the visco-elastic dynamics at current time t is calculated by using the hystory from time $t - T_{\mathrm{h}}$ up to time t, instead of considering all the values of the displacement history from $t = 0$ to t as follows:

$$AD^{\alpha}\mathbf{U}^{n+1} = A(\Delta t)^{-\alpha}\left[\mathbf{U}^{n-N_{\mathrm{h}}}|\ldots|\mathbf{U}^{n+1}\right]\begin{pmatrix} c_{N_{\mathrm{h}}+1}(\alpha) \\ \vdots \\ c_1(\alpha). \end{pmatrix}.$$

The effect of approximating the visco-elastic process in the range $[t - T_{\mathrm{h}}, t]$ of the displacement filed history is displayed in Fig. 8 in which the solution obtained with the full Grnwald-Letnikov approximation is compared with the solution obtained with a truncation with a memory horizon T_{h} for the displacement history. The advantage of truncating the approximation of the displacement history is to reduce the computational cost of the simulation. As shown in Fig. 8 this has an effect on the accuracy of the asymptotic solution for large time horizons.

5.4. Heat transfer in coupled thermo-visco-elastic dynamics

The numerical setup for this example is taken from [37]. Let $R = [0, L] \times [0, H]$ be a square domain in $\mathbb{R}^2$ occupied in its undeformed configuration by a visco-elastic material in a state of plane strain. The displacement $u =$

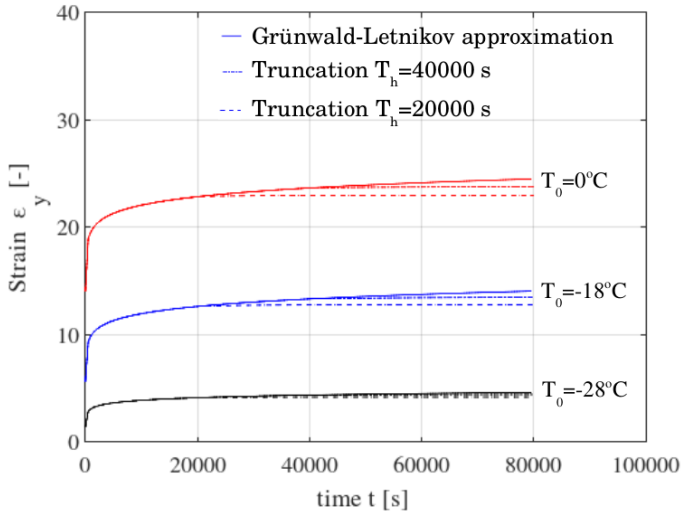

Figure 8: Solution of the relaxation problem for temperatures $T_0 = -28°\mathrm{C}, -18°\mathrm{C}, 0°\mathrm{C}$ obtained with the full Grnwald-Letnikov approximation (solid lines) and with a truncation of the displacement history of $T_\mathrm{h} = 40000$ s (dot dashed lines) and $T_\mathrm{h} = 20000$ s (dashed lines) .

$(u_x, u_y)^\mathrm{T}$ is such that u_x is zero on the right hand side. Loading is provided by a transient thermal analysis in which the left side has an imposed temperature $T_\mathrm{left} = 1$ K (all the quantities are adimensionalized as in [37]), which is suddenly applied at time zero and held constant. The other normalized parameters are the Young modulus $E = 100$ Pa, the Poisson coefficient $\nu = 0.4995$, the thermo-elastic coupling factor $\alpha_T = 0.25$, the initial temperature $T_0 = 0$ K, the thermal conductance $k = 10$ W/(m^{2}K), the heat capiacity $c = 1$, and the density $\rho = 0.1$ Kg/m^3, see [37]. The governing problem to be solved in $R \times [0, t_\mathrm{fin}]$ is:

$$-\mathrm{div}(\boldsymbol{\sigma}(\mathbf{u}, T)) = 0 \tag{26}$$

$$\rho c \frac{\partial T}{\partial t} + T_0 \beta \mathrm{div}\left(\frac{\partial \mathbf{u}}{\partial t}\right) = k \nabla^2 T. \tag{27}$$

The thermal stress $\boldsymbol{\sigma}$ is given by:

$$\boldsymbol{\sigma} = A\mathbf{G} D_{A,\alpha} \boldsymbol{\varepsilon} + (K\boldsymbol{\varepsilon} + \beta(T - T_0))\,\mathbf{I},$$

where $D_{A,\alpha}$ is the fractional-thermal derivative describing the thermal relaxation behavior is induced by the heat conduction equation. An Euler backward scheme for the time integration of the thermal problem has been adopted, in which the timestep is $\Delta t = 0.005$. Given the temperature T^n at the previous time t^n, let $m_k \leq n$ be the current value of the thermal clock. The visco-elastic problem consists in: find the current displacement $\mathbf{u}^{n+1}$, such that for all test function $\mathbf{v}$ holds:

$$\int_R \left((\Delta t)^{-\alpha(T^{m_k})} A(T^{m_k})\mathbf{G} + K\mathbf{I}\right) \boldsymbol{\varepsilon}(\mathbf{u}^{n+1}) : \boldsymbol{\varepsilon}(\mathbf{v})\, \mathrm{d}\mathbf{x} = \int_R \beta T^n \mathrm{div}(\mathbf{v})\, \mathrm{d}\mathbf{x} - \int_R (\Delta t)^{-\alpha(T^{m_k})} A(T^{m_k})\mathbf{G} \left(\sum_{j=m_k}^{n} c_{n+2-j}(\alpha(T^{m_k}))(\mathbf{u}^j)\right) : \boldsymbol{\varepsilon}(\mathbf{v})\, \mathrm{d}\mathbf{x}.$$

Then, given $\mathbf{u}^{n+1}$, solution of the previous problem, the temperature at the

current time T^{n+1} is such that, for each test function s:

$$\int_R \rho c \frac{\mathbf{u}^{n+1} - \mathbf{u}^n}{\Delta t} s \, \mathrm{d}\mathbf{x} + \int_R k \nabla T^{n+1} \cdot \nabla s \, \mathrm{d}\mathbf{x} + \int_R \beta T_0 \mathrm{div} \left(\frac{\mathbf{u}^{n+1} - \mathbf{u}^n}{\Delta t} \right) s \, \mathrm{d}\mathbf{x}.$$

For the simulation $\mathbb{P}^2$ lagrangian triangular elements have been used to approximate the displacement field and $\mathbb{P}^1$ lagrangian trianguar elements have been used to approximate temperature.

5.4.1. Case I: Fractional visco-elastic parameters $A = E$, $\alpha = \{0, 0.1, 0.25\}$

In this first example, the material parameters for the fractional derivative are taken as $A = E$ fixed and the fractional exponent is varied as $\alpha = \{0, 0.1, 0.25\}$. In Fig. 9, the contour plots of temperature $T(x, y, t)$ and the horizontal component $\sigma_x(x, y, t)$ of the stress tensor for the initial and final time are shown. Temperature is diffusing linearly inside the region from the left lateral side of the square. In Fig. 11, the spatial evolution of the temperature profile and thermal stress component σ_{xx} are plotted along the central line of the square $\{y = H/2\}$ for subsequent times in the thermo-elastic case ($\alpha = 0$). In Fig. 11, the spatial evolution of the thermal stress component σ_{xx} along the central line of the square $\{y = H/2\}$ is shown for subsequent times and for different values of the fractional exponent $\alpha = 0.1, 0.25$.

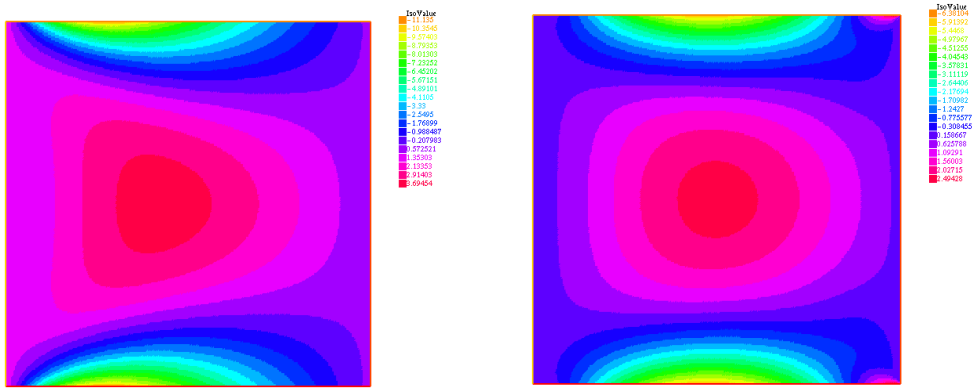

Figure 9: Contour plots of the horizontal component σ_{xx} of the stress at initial and final time ($\alpha = 0$).

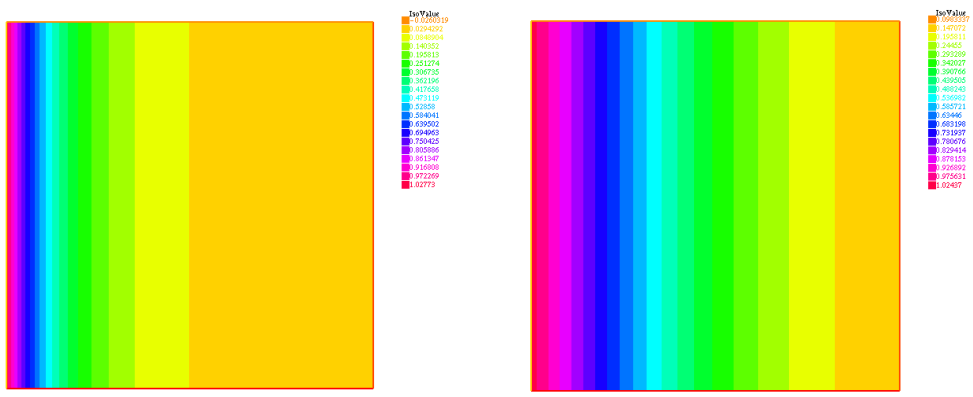

Figure 10: Contour plots of the temperature T at initial and final time ($\alpha = 0$).

5.4.2. Case II: Fractional visco-elastic parameters A, α temperature dependent

In this example, the material functions $A(T)$ and $\alpha(T)$ are considered as functions of temperature T as:

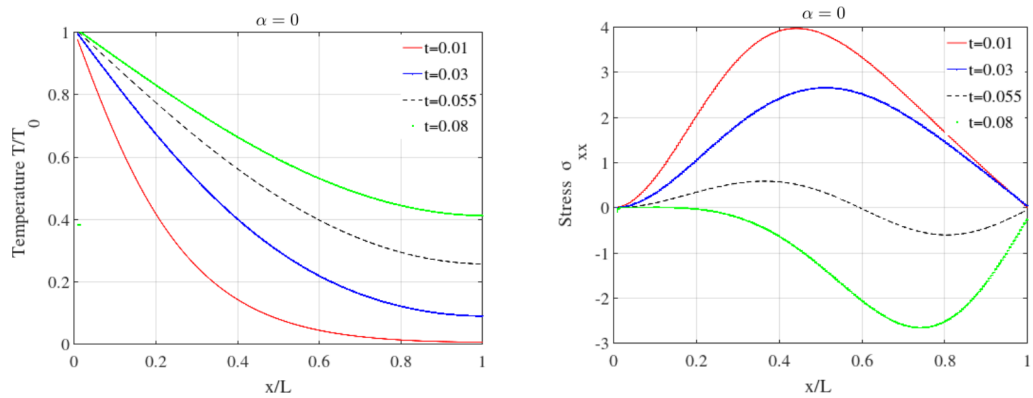

Figure 11: Numerical results of the spatial evolution of the temperature T (left) and stress component σ_{xx} (right) along the line $\{y = H/2\}$ at different normalized times for the elastic limit $\alpha = 0$.

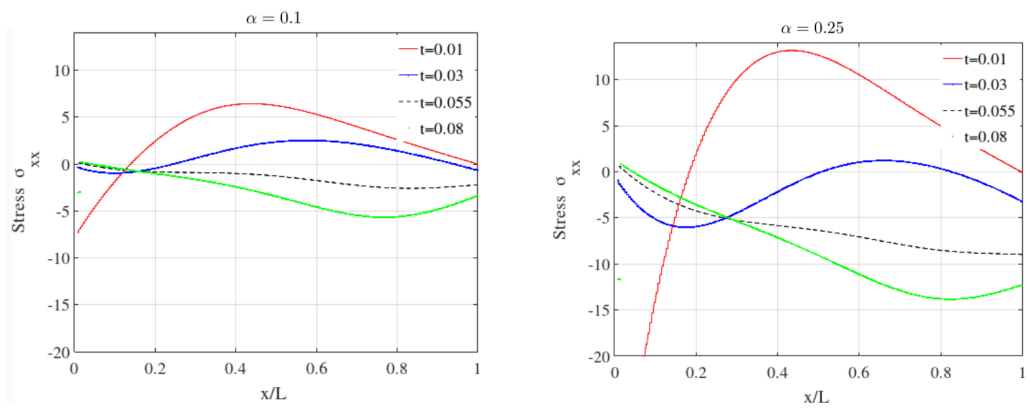

Figure 12: Numerical simulation of the the spatial evolution of the stress component σ_{xx} along the line $\{y = H/2\}$ at different normalized times for different values of the fractional exponent $\alpha = \{0.1, 0.25\}$.

$$A(T) = \begin{cases} 10E & \text{if } T \leq T^*, \\ 0.1E & \text{if } T > T^* \end{cases}, \qquad \alpha(T) = \begin{cases} 0.05 & \text{if } T \leq T^*, \\ 0.25 & \text{if } T > T^* \end{cases}. \tag{28}$$

where $T^* = 0.5$. The temporal evolution of the stress component σ_{xx} is shown in Fig. 13 for three points in the square domain $R = [0, L] \times [0, H]$, respectively $P_1 = (L/4, H/2)$, $P_2(L/2, H/2)$ and $P_3 = (3L/4, H/2)$ for the cases $\alpha = 0, A = E$ (thermo-elastic case) and for α and A as in Eq. (29).

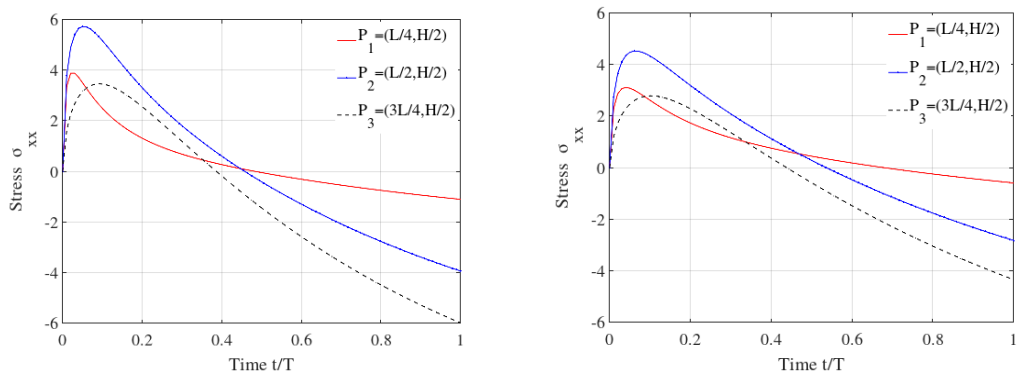

Figure 13: Numerical solution of the temporal evolution of the horizontal component σ_{xx} of the stress on different points $P_1 = (L/4, H/2)$, $P_2(L/2, H/2)$ and $P_3 = (3L/4, H/2)$ of the square domain $R = [0, L] \times [0, H]$ for the thermo-elastic case $\alpha = 0, A = E$ (left) and for α and A as in Eq. (29) (right).

6. Conclusions

A novel finite element computational framework for the simulation of coupled thermo-visco-elasticity problems in thermo-rehologically complex materials with memory has been proposed. The visco-elastic constitutive law is based on fractional calculus. Fractional calculus and the theory of Mittag-Leffler special functions allow an accurate description of the time relaxation behaviour of the material. The fractional parameters of the model are assumed to be temperature dependent. An internal material clock has therefore been introduced to model the thermo-rheological complexity of materials in which the classical time-temperature superposition principle does not apply. The model is able to represent the phase transition experienced by the relaxation modulus as a function of temperature. The numerical treatment of the fractional derivative has been done via the Grnwald-Letnikov approximation which leads to an additional load vector which represents the memory of the material in the discretized system of equations resulting from the finite element formulation.

The poposed model has been implemented in the finite element software FreeFem++ [36] and has been used to solve numerically various test cases, namely: (i) the free vibrations of a visco-elastic rod; (ii) creep tests; (iii) heat transfer in coupled thermo-visco-elastic dynamics. The proposed model has been validated against creep and relaxation tests conducted at different temperatures on EVA, a real visco-elastic material which is a polymer used as encapsulant for solar cells. With the present computational tool avail-

able, further developments may regard the simulation of thermo-visco-elastic phenomena observed in experiments, opening the possibility to accurately simulate with the finite element method any arbitrary rheologically complex material for any application and problem geometry.

Acknowledgements

The support from the Italian Ministry of Education, University and Research (MIUR) to the Research Project of Relevant National Interest (PRIN 2017) "XFAST-SIMS: Extra-fast and accurate simulation of complex structural systems" (CUP: D68D19001260001) is gratefully acknowledged.

References

[1] A. F. Bower (2009) Applied Mechanics of Solids. CRC Press, 1 edition.

[2] M. Pander, S. Dietrich, S. H. Schulze, U. Eitner, and M. Ebert (2011) Thermo-mechanical assessment of solar cell displacement with respect to the visco-elastic behaviour of the encapsulant. 2011 12th Intl. Conf. on Thermal, Mechanical Multi-Physics Simulation and Experiments in Microelectronics and Microsystems: 1–6.

[3] M. Kntges, R. Brendel, U. Eitner, S. Kajari-Schrder (2010) Non-linear mechanical properties of ethylene-vinyl acetate (eva) and its relevance

to thermomechanics of photovoltaic modules. In 25th European Photovoltaic Solar Energy Conference, 4AV.3.115.

[4] M. Paggi, A. Sapora (2015) An accurate thermovisco-elastic rheological model for ethylene vinyl acetate based on fractional calculus. International Journal of Photoenergy: 7.

[5] A. Valenza, M. Di Paola, A. Pirrotta (2011) Visco-elastic behavior through fractional calculus: An easier method for best fitting experimental results. Mechanics of Materials, 43:799?806.

[6] M. Enelund, G.A. Lesieutre (1999) Time domain modeling of damping using anelastic displacement fields and fractional calculus. International Journal of Solids and Structures, 36(29):4447– 4472.

[7] R. L. Bagley (1991) The thermorheologically complex material. International Journal of Engineering Science, 29(7): 797–806.

[8] R.C. Koeller (1984) Application of fractional calculus to the theory of visco-elasticity. J. Appl. Mech., 51: 229–307.

[9] L. Gaul, A. Schmidt (2002) Finite element formulation of visco-elastic constitutive equations using fractional time derivatives. Nonlinear Dynamics, 29(1): 37–55.

[10] K. Adolfsson, M. Enelund (2003) Fractional derivative visco-elasticity at large deformations. Nonlinear Dynamics, 33(3): 301–321.

[11] M. Fabrizio (2014) Fractional rheological models for thermomechanical systems. Dissipation and free energies. Fractional Calculus and Applied Analysis, 17(1): 206–223.

[12] A. Ding, S. Li, J. Wang, L. Zu (2015) A three-dimensional thermo-visco-elastic analysis of process-induced residual stress in composite laminates. Composite Structures, 129: 60– 69.

[13] S. B. Emri, I. M. Gergesova, B. Zupani (2010) The closed form ttp shifting (cfs) algorithm. Journal of Rheology, 55(1).

[14] A. D. Freed, A. I. Leonov (2002) A thermodynamic theory of solid visco-elasticity. part 1: Linear visco-elasticity.

[15] W. G. Glckle, T. F. Nonnenmacher (1994) Fractional relaxation and the time-temperature superposition principle. Rheologica Acta, 33(4):337–343.

[16] G. A. Holzapfel, J. C. Simo (1996) A new visco-elastic constitutive model for continuous media at finite thermomechanical changes. International Journal of Solids and Structures, 33(20): 3019 – 3034.

[17] R. K. Saxena, A. M. Mathai, H. J. Haubold (2011) Mittag-leffler functions and their applications. Journal of Applied Mathematics, (298628).

[18] H. F Brinson (2008) Polymer engineering science and visco-elasticity: an introduction, Springer.

[19] F. Mainardi (2010) An Introduction to Mathematical Models. Imperial College Press, London, UK.

[20] A.C. Pipkin (2012) Lectures on Viscoelasticity Theory. Applied Mathematical Sciences. Springer New York.

[21] W. G. Glckle, T. F. Nonnenmacher (1994) Fractional relaxation and the time-temperature superposition principle. Rheologica Acta, 33(4):337–343.

[22] R.M. Christensen (2013) Theory of Viscoelasticity: Second Edition. Dover Civil and Mechanical Engineering. Dover Publications.

[23] S. W. Katicha, G. W. Flintsch (2012) Fractional visco-elastic models: master curve construction, interconversion, and numerical approximation. Rheologica Acta, 51(8):675–689.

[24] J. D. Ferry, M. L Williams (1952) Second approximation methods for determining the relaxation time spectrum of a visco-elastic material. Journal of Colloid Science, 7(4): 347 – 353.

[25] T. Voigtmann (2014) Nonlinear glassy rheology. Current Opinion in Colloid and Interface Science, 19(6): 549 – 560.

[26] M. Kntges, H. Altenbach, U. Eitner, S. Kajari-Schrder (2011) Thermal stress and strain of solar cells in photovoltaic modules. Advanced Structured Materials, 15:453–468.

[27] K. A. Kamran, H. M. Anastasia (2012) Fully coupled heat conduction and deformation analyses of nonlinear visco-elastic composites. Composite Structures, 94(6):2025–2037.

[28] M. A. Ezzat, A. A. El-Bary (2015) Memory-dependent derivatives theory of thermo-visco-elasticity involving two-temperature. Journal of Mechanical Science and Technology, 29(10):4273–4279.

[29] W. Zhang, S. Nobuyuki (2001) Fe formulation for the visco-elastic body modeled by fractional constitutive law. Acta Mechanica Sinica, 17(4):354–365.

[30] Y. T. H. Jianfei, R. Scherer, S. L. Kalla (2011) The Grnwald-Letnikov method for fractional differential equations. Comp. Math. Appl., 62(3):902–917.

[31] L. Morini, A. Piccolroaz (2015) Boundary integral formulation for interfacial cracks in thermodiffusive bimaterials. Proc. R. Soc. A 373: 20150284.

[32] A. Carpinteri, P. Cornetti, A. Sapora (2011) A fractional calculus approach to nonlocal elasticity. The European Physical Journal Special Topics 193(1).

[33] M. Zingales, M. Di Paola, A. Carpinteri, A. Sapora, P. Cornetti (2009) Fractional calculus in solid mechanics: local versus non-local approach. Physica Scripta, TI36:014003–014010.

[34] M. Di Paola, A. Pirrotta, A. Valenza (2011) Visco-elastic behavior through fractional calculus: An easier method for best fitting experimental results. Mechanics of Materials, 43(12):799–806.

[35] G. Alba , M. Di Paola (2016) Fractional Thermovisco-elastic materials. Meccanica dei Materiali e delle Strutture, 6(2):1–10.

[36] F. Hecht (2012) New development in FreeFem++. Journal of Numerical Mathematics, 20(3-4):251–265.

[37] R. L. Taylor (2014) FEAP - Finite Element Analysis Program. University of California, Berkeley.

[38] M. Di Paola, M. Zingales (2013) The Multiscale Stochastic Model of Fractional Hereditary Materials (FHM). Procedia IUTAM, 6:50–59.

[39] O. Baglieri, E. Santagata, A. Sapora P. Cornetti, A. Carpinteri (2017) Fractional Viscoelastic Modeling of Antirutting Response of Bituminous Binders. Journal of Engineering Mechanics, 143(5):D4016002.

[40] A. Sapora, P. Cornetti, A. Carpinteri, O. Baglieri, E. Santagata (2016) The use of fractional calculus to model the experimental creep-recovery behavior of modified bituminous binders. Materials and Structures, 49:45–55.